Chinese Chemical Letters 33 (2022) 1572–1576

Contents lists available at ScienceDirect

Chinese Chemical Letters

journal homepage: www.elsevier.com/locate/cclet

Specific tracking of monoamine oxidase A in heart failure models by a far-red fluorescent probe with an ultra large Stokes shift

Xinming Li[a], Donglei Shi[a], Yihe Song[a], Yixiang Xu[a], Ying Gao[b], Wenjing Qiu[a], Xin Chen[a], Xiaokang Li[a], Yunyuan Huang[a], Yanjun Feng[a], Baoli Li[a,*], Yuan Guo[b,*], Jian Li[a,c,d,e,*]

[a] State Key Laboratory of Bioreactor Engineering, Shanghai Key Laboratory of New Drug Design, School of Pharmacy, East China University of Science and Technology, Shanghai 200237, China
[b] Key Laboratory of Synthetic and Natural Functional Molecule of the Ministry of Education, College of Chemistry and Materials Science, Northwest University, Xi'an 710127, China
[c] Frontiers Science Center for Materiobiology and Dynamic Chemistry, East China University of Science and Technology, Shanghai 200237, China
[d] College of Pharmacy and Chemistry, Dali University, Dali 671000, China
[e] Clinical Medicine Scientific and Technical Innovation Center, Shanghai Tenth People's Hospital, Tongji University School of Medicine, Shanghai 200092, China

ARTICLE INFO

Article history:
Received 2 June 2021
Revised 18 August 2021
Accepted 24 August 2021
Available online 30 August 2021

Keywords:
Heart failure
Monoamine oxidase A
Oxidative stress
Fluorescent probe
Far-red emission
Diagnosis

ABSTRACT

Monoamine oxidase A (MAO-A) is a prominent myocardial source of reactive oxygen species (ROS), and its expression and activity are strongly increased in failing hearts. Therefore, accurate evaluation of MAO-A activity in cardiomyocytes is of great importance for understanding its biological functions and early diagnosing the progression of heart failure. However, so far, there is no report on the fluorescent diagnosis of heart failure by a specific probe for MAO-A. In this work, two far-red emissive fluorescent turn-on probes (KXS-M1 and KXS-M2) for the highly selective and sensitive detection of MAO-A were fabricated. Both probes exhibit good response to MAO-A, one of which, KXS-M2, performs better than the other one in terms of a fluorescence increment and sensitivity. Using the pioneering probe KXS-M2, specific fluorescence imaging of MAO-A in glucose-deprived H9c2 cardiac cells, zebrafish and isoprenaline-induced failing heart tissues was achieved, proving that KXS-M2 can serve as a powerful tool for the diagnosis and treatment of heart failure.

Heart failure (HF) is an inevitable terminal stage for most cardiac diseases. This disease is known to be associated with multifarious etiologies and an estimated 64.3 million people are suffering from it so far. Remarkable advances in the treatment and prevention of HF have been made in the past two decades, while its incidence and prevalence rates still continue to increase due to the global demography of aging [1]. As a consequence, there is still an urgent need to continue to investigate the diagnosis, pathogenesis, and treatment of HF.

Among the mechanisms involved in the etiopathogenesis of HF, substantial evidence indicates that overproduction of reactive oxygen species (ROS) and the resulting oxidative damage play an important role in the initiation and progression of this disease [2–5]. Monoamine oxidases (MAOs) are outer mitochondrial membrane-located flavoenzymes, which are responsible for catalyzing the oxidative deamination of neurotransmitters with the generation of aldehydes and hydrogen peroxide. There exist two isoforms of MAOs termed MAO-A and MAO-B in mammals. The two enzymes share high structural homology and the same catalytic mechanism, but differ significantly in their biological functions [6]. MAO-A is a classical therapeutic target for depression [7,8], while, in recent years, a growing number of researches revealed that the protein expression and enzymatic activity of MAO-A increased significantly in pathological cardiac hypertrophy and HF [9–11]. As a prominent myocardial source of ROS, the overexpressed MAO-A leads to the excessive production of ROS and accumulation of reactive aldehydes in heart tissue, and subsequently activates a battery of signal pathways involved in the initiation and progression of HF [12–14]. Thus, we propose that MAO-A may serve as a potential biomarker to predict HF earlier, and development effective methods for monitoring MAO-A activity could facilitate the diagnosis and treatment of HF.

Fluorescence-based detecting techniques have been grown up to be an important tool in investigating disease-related biomark-

* Corresponding authors.
E-mail addresses: libaolilibaoli@163.com (B. Li), guoyuan@nwu.edu.cn (Y. Guo), jianli@ecust.edu.cn (J. Li).

https://doi.org/10.1016/j.cclet.2021.08.114
1001-8417/

ers [15,16]. So far, a great number of small-molecular fluorescent probes have been developed for the detection of MAOs [17–19]. Among them, specific probes capable of distinguishing MAO-A from MAO-B has received increasing interest and great progress has also been made, as the two isoforms of MAOs are associated with different diseases [20,21]. One of the notable design strategies for them is to employ the characteristic structure of clorgiline, a MAO-A specific inhibitor, as a targeting moiety, which was first reported by Ma's group [22]. Li and coworkers then introduced this enzyme-recognition moiety into the dicyanomethylene-4*H*-pyran (DCM) fluorophore to further construct a MAO-A-specific near-infrared fluorescent probe, and achieved the selective visualization of MAO-A activity *in vivo* [23]. Very recently, the first two-photon fluorescent probe for MAO-A was disclosed by Huang's group, and successfully applied to *in vitro* and *in vivo* imaging [24]. Although several robust probes for MAO-A imaging have been reported, probes with far-red/near-infrared emission and large Stokes shift which is more suitable for bioimaging of MAO-A in complicated biosystems are still inadequate [25–28]. Moreover, imaging methods for specific MAO-A determination in the pathology of HF is in shortage as well.

To this end, we fabricated two novel far-red-emission fluorescent probes KXS-M1 and KXS-M2 for specific tracking of MAO-A, which were designed by using propylamine as a recognition moiety and chlorine-substituted dicyanoisophorone (DCF) as the fluorophore [29,30]. After being incubated with MAO-A, the free DCF fluorophore was liberated based on amine oxidation and β-elimination mechanism (Scheme 1). The synthetic routes to the probes and the characterization could be found in Supporting information.

First, we investigated their ability to selectively detect MAO-A. The changes of fluorescence intensity were evaluated after incubation of the probes with the recombinant human MAOs in the PBS buffer (10 mmol/L, pH 7.4, 20% DMSO). The fluorescence signals of probe KXS-M1 and KXS-M2 were trigged on by MAO-A with a ~80 and ~195-fold increase of the emission intensity, respectively. However, MAO-B just caused a ~4 and ~8-fold fluorescence increases of KXS-M1 and KXS-M2, respectively (Fig. S1 in Supporting information). The selectivity for MAO-A over MAO-B was calculated to be 20-fold for KXS-M1 and 24.4-fold for KXS-M2. These results indicated that both KXS-M1 and KXS-M2 exhibit high specificity to MAO-A. Considering the higher sensitivity of KXS-M2 for MAO-A than KXS-M1, KXS-M2 was selected as the fluorescence probe for the further study.

The UV-vis absorption spectrum of the KXS-M2 solution incubated with MAO-A or MAO-B was tested (Fig. 1A). KXS-M2 exhibits a strong absorption band centered at 410 nm, and this absorption maximum decreased after the addition of MAO-A. Meanwhile, a significant increase in the absorption band centered at 500 nm appeared, which was consistent with that of DCF, demonstrating that the MAO-A triggered the release of free DCF. Simultaneously, a remarkable fluorescence intensity enhancement at 670 nm was observed (Fig. S1). While, just a faint increase of the absorbance at 500 nm and fluorescence intensity at 670 nm were observed when KXS-M2 was incubated with MAO-B. To verify the sensing mechanism, the high-performance liquid chromatography (HPLC) experiment was performed. As shown in Fig. S2 (Supporting information), the retention time for free KXS-M2 and DCF was 7.02 min and 26.76 min, respectively. After incubation with MAO-A, the peak for KXS-M2 decreased, while a new peak appeared which was coincide with the retention time of free DCF, indicating that KXS-M2 could be hydrolyzed by MAO-A to liberate the fluorophore DCF accompanied with a turn-on fluorescent signal. Together, probe KXS-M2 could serve as a "turn-on" fluorescent probe for MAO-A detection. Furthermore, the far-red emission of KXS-M2 toward MAO-A with an ultra large Stokes shift (170 nm) was very appropriate for bioimaging applications.

We then evaluated the time dependent emission spectra of KXS-M2 toward MAO-A (Fig. S3 in Supporting information), the intensity at 670 nm enhanced gradually over incubation time and reached a plateau within 240 min. Subsequently, the optical responses of the probe to various concentrations of MAO-A were determined (Fig. 1B). An obvious increase in fluorescence intensity was observed with the continuous increasing concentration of MAO-A. Plotting the fluorescence intensity versus concentrations of MAO-A ranging from 0 to 10 μg/mL gave a good linear relationship (inset in Fig. 1B). According to the 3σ/k method, the detection limit of MAO-A was calculated to be 9.8 ng/mL, indicating that KXS-M2 could detect the trace amounts of intracellular MAO-A. In addition, the kinetic parameters for the MAO-A-activated reaction of probe KXS-M2 were investigated according to the Lineweaver–Burk equation. The Michaelis constant (K_m) and the maximum of the initial reaction rate (V_{max}) were calculated to be 12.1 μmol/L and 4.34 nmol mg^{-1} min^{-1}, respectively (Fig. S4 in Supporting information). The low K_m value indicates a strong affinity between KXS-M2 and MAO-A, demonstrating that the probe is a good substrate for MAO-A.

Next, we determined the selectivity of KXS-M2 towards MAO-A in the presence of various potential biological interfering species, including MAO-B, cellulase, β-galactosidase, lysozyme, phosphatase, trypsin, DTT, GSH, Hcy, and Cys. KXS-M2 only exhibited an obvious enhancement in the presence of MAO-A (Fig. 1C). And this fluorescence enhancement was sharply suppressed by clorgiline (CL) [31], a specific MAO-A inhibitor (Fig. S5 in Supporting information). Then the fluorescence response of KXS-M2 to MAO-A at the pH ranging from 4.0 to 10.0 were also investigated (Fig. S6 in Supporting information). The probe itself exhibited a negligible fluorescence change in the tested pH range. However, the reaction system displayed remarkable fluorescence enhancement after incubation with MAO-A above the pH range of 6.5−9.5. Overall, these results indicated that KXS-M2 exhibited good selectivity and high practical value for imaging of MAO-A in physiological conditions.

To demonstrate the probe could be used to image intracellular MAO-A, the cell cytotoxicity of KXS-M2 was evaluated with SH-SY5Y, HepG2 and H9c2 cells. Results showed that the cells can be maintained viability up to 95% even after incubation with 10 μmol/L of KXS-M2 for 24 h (Fig. S7 in Supporting information), demonstrating that the probe is suitable for imaging in living cells. Numerous studies have reported that the expression levels of MAO-A and MAO-B are elevated in human-derived SH-SY5Y and HepG2 cell lines, respectively [22,24,27]. After treatment with 5 μmol/L KXS-M2 for 3 h, a prominent red fluorescent signal was observed in SH-SY5Y cells and this fluorescence signal intensity was significantly decreased by the MAO-A inhibitor CL. Conversely, pretreating the cells with the MAO-B inhibitor pargyline (PL) only caused a slight fluorescence change compared to CL. On the other hand, HepG2 cells treatment with KXS-M2 failed to generate any fluorescence enhancement (Figs. 1D and E). The above results indicated that KXS-M2 can specifically imaging intracellular MAO-A.

MAO-A is responsible for catalyzing the oxidative deamination of serotonin (5-HT) and norepinephrine (NE) in the heart, but produces H_2O_2 and relative aldehydes as by-products during the degradation process. Although the overactivation of MAO-A has been suggested to link to HF, the direct evidence is inadequate probably due to the lack of detection methods for real-time monitoring of MAO-A activity in the HF process. Consequently, having confirmed the efficacy and specificity of KXS-M2 in living cells, we attempted to monitor MAO-A activity in a cellular model of HF.

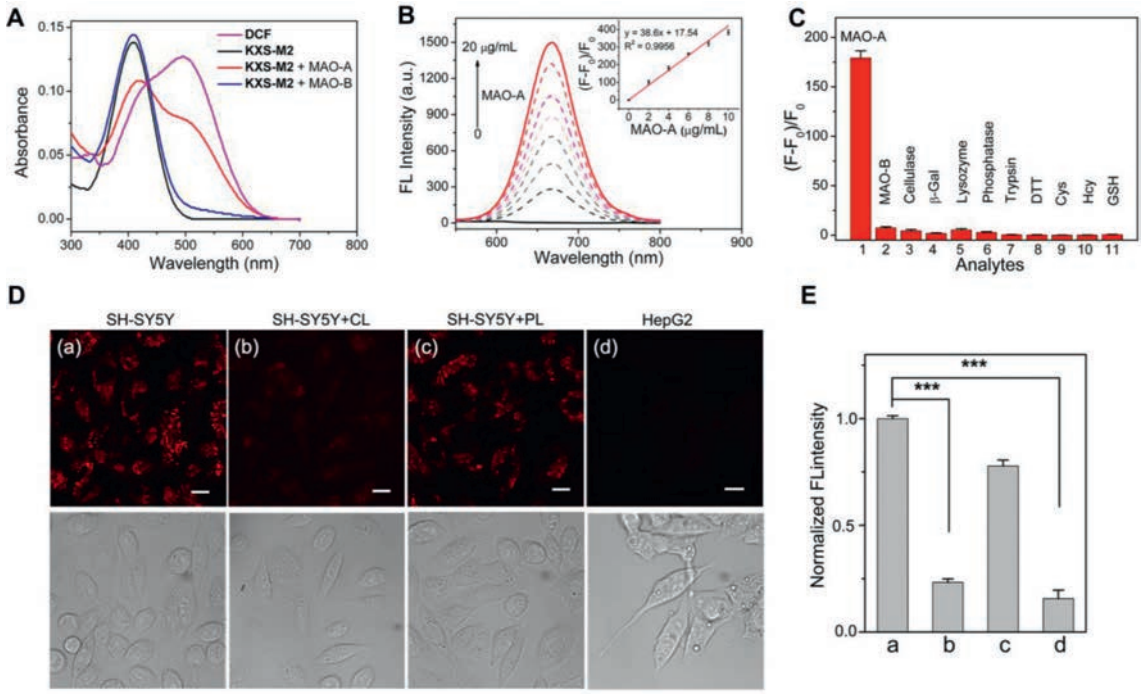

Fig. 1. (A) UV-vis absorption spectra of KXS-M2 (5 μmol/L) after reaction with MAO-A or MAO-B (10 μg/mL). (B) Fluorescence emission spectra of KXS-M2 (5 μmol/L) after reaction with MAO-A (0-20 μg/mL) for 3 h (λ_{ex} = 500 nm). (C) Fluorescence changes of KXS-M2 (5 μmol/L) upon addition of various analytes for 3 h (λ_{ex} = 500 nm). (D) SH-SY5Y and HepG2 cells were pretreated with or without an inhibitor (10 μmol/L CL/PL) for 1 h, and then were further stained with KXS-M2 (5 μmol/L) for 3 h. (E) Relative fluorescence intensity measurements from image (D) by ImageJ software. λ_{ex} = 488 nm, λ_{em} = 625-725 nm. Scale bar: 20 μm. Error bars represent standard deviation (n = 3). Significance differences ($^{***}P < 0.001$) are analyzed with two-sided Student's t-test.

Ischemic heart disease is the main cause of HF [32]. Glucose deprivation (GD) is widely used in generating cell models of ischemia [33,34]. We incubated the H9c2 embryonic rat cardiac cells with glucose-free DMEM for 0, 12, 24 and 36 h, and then determined the MAO-A activity by KXS-M2 staining. The fluorescence intensity of KXS-M2 increased significantly with the extension of GD time (Figs. 2A and B). Next, we evaluated the expression levels of MAO-A in the cells by Western blot analysis (Fig. 2C). The results further confirmed the reliability of KXS-M2 for imaging MAO-A in living cells. Considering that MAO-A is located in the outer-membrane of mitochondria, we then performed the fluorescence colocalization assays to investigated the subcellular localization of KXS-M2 in H9C2 cells (Fig. S8 in Supporting information). After the cells were incubated with KXS-M2 and Mito-Tracker Green or Lyso-Traker Geen, the overlap coefficient (R) was calculated to be 0.7370 for mitochondria and 0.7354 for lysosome. Such non-selective imaging of MAO-A in mitochondria maybe attributed to the diffusion of the generated fluorophore from the outer-membrane of mitochondria after a longtime incubation.

Given the far-red emission of KXS-M2, the capability of KXS-M2 for detecting MAO-A activity in living zebrafish and in failing heart tissues was subsequently investigated (Fig. 3). Zebrafish incubated with KXS-M2 alone for 3 h exhibited strong red fluorescence. However, when pretreated with CL for 1 h, the fluorescence signal was sharply suppressed (Fig. 3G). Pretreating the zebrafish with PL only caused an inappreciable fluorescence change compared to CL (Fig. 3H), demonstrating that KXS-M2 can be used to selectively detect MAO-A activity *in vivo*.

For failing heart tissue imaging, we generated the mouse HF model by subcutaneous injection of isoproterenol (ISO) (Approved by the Institutional Animal Care and Use Committees of Tongji University). ISO is a nonselective beta-adrenergic agonist and is widely used to establish mouse models to mimic stress-induced cardiomyopathy and advanced HF in humans [35]. Heart tissue

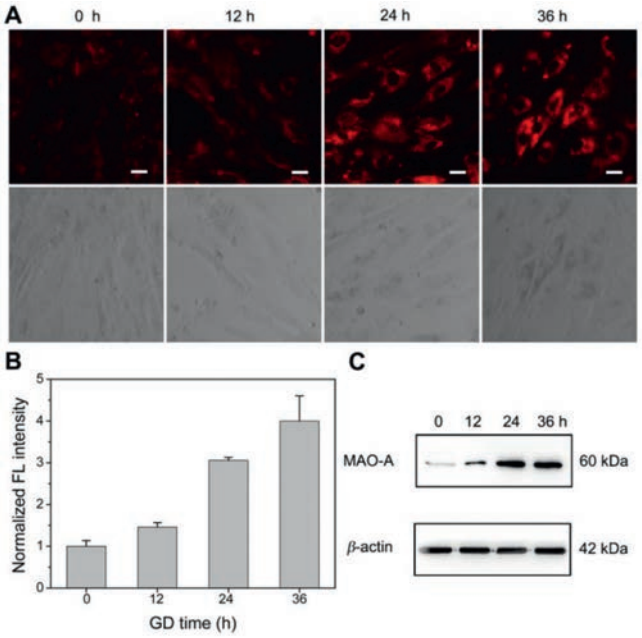

Fig. 2. (A) Confocal fluorescence bioimaging of MAO-A activity by KXS-M2 in glucose-deprived H9c2 cardiac cells. (B) Relative fluorescence intensity measurements from image (A) by ImageJ software. (C) Western blots of MAO-A in glucose-deprived H9c2 cardiac cells. β-Actin is a loading control for the blot. λ_{ex} = 488 nm, λ_{em} = 625-725 nm. Scale bar: 20 μm.

slices from the normal saline (NS) group and ISO group were prepared and immediately incubated with KXS-M2 (5 μmol/L) for 3 h at 37 °C. Meanwhile, H&E staining was also performed to identify the morphological changes of cardiomyocytes after ISO treat-

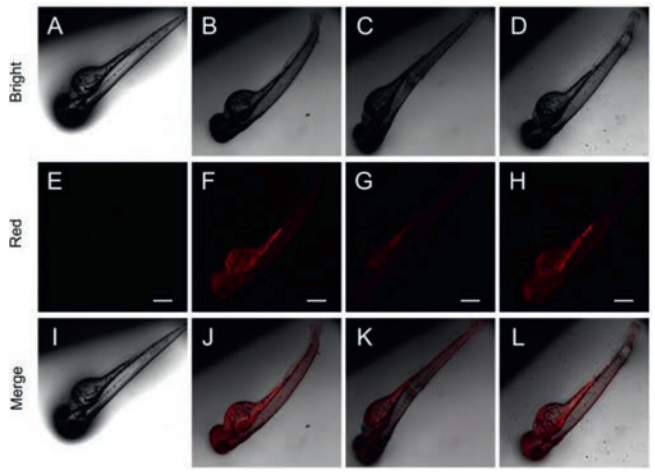

Fig. 3. Fluorescence images in zebrafish with KXS-M2 for selective detection of MAO-A. (A, E and I) Only zebrafish; (B, F and J) Zebrafish were stained with only probe KXS-M2 (10 μmol/L) for 3 h; (C, G and K) Zebrafish were pretreated with CL (10 μmol/L) for 1 h and then stained with KXS-M2 (10 μmol/L) for 3 h; (D, H and L) Zebrafish were pretreated with PL (10 μmol/L) for 1 h and then stained with KXS-M2 (10 μmol/L) for 3 h. Scale bar: 300 μm.

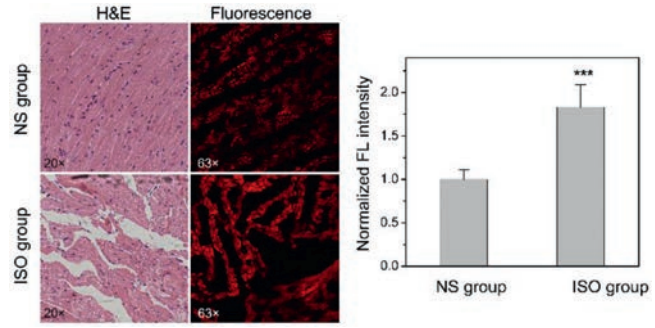

Fig. 4. H&E staining and fluorescence imaging of MAO-A in heart tissue of mouse models, and the relative fluorescence intensity measurements of heart tissues by ImageJ software. Error bars represent the standard deviation (± S.D.) with $n = 5$. Significance differences ($^{***}P < 0.001$) are analyzed with two-sided Student's t-test.

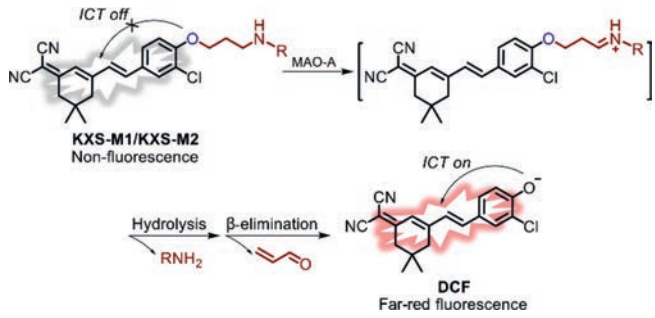

Scheme 1. Proposed sensing mechanism of probe KXS-M1/KXS-M2 toward MAO-A.

ment (Fig. 4). The NS group showed regular arrangement in cardiac muscle fibers, whereas the ISO group exhibited serious myofibrillar disorganization, indicating that ISO had induced significant cardiac impairments. Correspondingly, the fluorescence intensity in the ISO group was about 2-fold higher than those in the NS group, which suggested that the activity of MAO-A enhanced with HF. Taken together, the results of monitoring the relationship between MAO-A activity and progression of HF proposed that the increased MAO-A activity may serve as a potential biomarker for the diagnosis of HF.

Finally, to evaluate whether KXS-M2 can serve as an effective tool to test the efficacy of drugs for the treatment of HF, we measured the fluorescence intensity changes in H9c2 cells under GD model with or without the addition of an anti-HF drug, empagliflozin (EMPA) [36]. After stained with KXS-M2, an obvious red fluorescence signal was observed in the cells exposed to 36 h of GD, whereas, EMPA dose-dependently reduced the fluorescence intensity (Figs. S9A and B in Supporting information). A cell viability assay was also performed to confirm the cardioprotective properties of EMPA under GD conditions. Results indicated that EMPA exerted prominent protective effects on cell viability in the GD model (Fig. S9C in Supporting information). Taken together, these results further demonstrated that the MAO-A activity is closely related to the progression of HF, and the probe KXS-M2 can be utilized for future research on the diagnosis and treatment of HF.

In summary, two novel far-red fluorescent probes based on a chlorine-substituted dicyanoisophorone, KXS-M1 and KXS-M2, have been designed and synthesized to investigate MAO-A activity in the pathology of HF. Both probes are easy to be synthesized and exhibit high sensitivity and selectivity for MAO-A. In particular, KXS-M2 exhibits an ultra large Stokes shift, a prominent far-red emission, significant fluorescent enhancement and low cytotoxicity. With our probe KXS-M2, the accurate detection of MAO-A activity in glucose-deprived H9c2 cardiac cells, zebrafish and ISO-induced failing heart tissues have been achieved *via* confocal fluorescence imaging. Furthermore, our results indicate that the progression of HF is positively related to the activities of MAO-A, suggesting that MAO-A may act as a potential indicator of HF.

Declaration of competing interest

The authors declare that they have no known competing financial interests or personal relationships that could have appeared to influence the work reported in this paper.

Acknowledgments

This work was supported by the National Natural Science Foundation of China (Nos. 22037002, 22007032 and 21977082), the National Mega-project for Innovative Drugs of China (No. 2019ZX09721001-004-003), the Chinese Postdoctoral Science Foundation, China (No. 2019M660083), the Shanghai Sailing Program, China (No. 20YF1411200).

Supplementary materials

Supplementary material associated with this article can be found, in the online version, at doi:10.1016/j.cclet.2021.08.114.

References

[1] A. Groenewegen, F.H. Rutten, A. Mosterd, Eur. J. Heart Fail. 22 (2020) 1342–1356.
[2] C.D. Kemp, J.V. Conte, Cardiovasc. Pathol. 21 (2012) 365–371.
[3] D. Sorescu, K.K. Griendling, Congest. Heart Fail. 8 (2002) 132–140.
[4] H. Tsutsui, S. Kinugawa, S. Matsushima, Am. J. Physiol. Heart Circ. Physiol. 301 (2011) 2181–2190.
[5] A. van der Pol, W.H. van Gilst, A.A. Voors, P. van der Meer, Eur. J. Heart Fail. 21 (2019) 425–435.
[6] K. Chen, J.C. Shih, Adv. Pharmacol. 42 (1997) 292–296.
[7] M.E. Thase, M.H. Trivedi, A.J. Rush, Neuropsychopharmacology 12 (1995) 185–219.
[8] K. Domschke, C. Hohoff, L.S. Mortensen, Prog. Neuro-Psychopharmacol. Biol. Psychiatry 32 (2008) 224–228.
[9] N. Kaludercic, E. Takimoto, T. Nagayama, Circ. Res. 106 (2010) 193–202.
[10] N. Kaludercic, A. Carpi, R. Menabo, F. Di Lisa, Biochim. Biophys. Acta 1813 (2011) 1323–1332.
[11] M.E. Manni, S. Rigacci, E. Borchi, Oxid. Med. Cell. Longev. 2016 (2016) 4375418.
[12] D. Maggiorani, N. Manzella, D.E. Edmondson, Oxid. Med. Cell. Longev. 2017 (2017) 3017947.
[13] Y. Santin, L. Fazal, Y. Sainte-Marie, Cell Death Differ. 27 (2020) 1907–1923.
[14] Y. Santin, J. Resta, A. Parini, Ageing Res. Rev. 66 (2021) 101256.
[15] J. Zhang, X. Chai, X.P. He, Chem. Soc. Rev. 48 (2019) 683–722.
[16] D. Yue, M. Wang, F. Deng, Chin. Chem. Lett. 29 (2018) 648–656.

[17] H.H. Qin, L.L. Li, K. Li, Chin. Chem. Lett. 30 (2019) 71–74.
[18] J. Zhou, P. Jangili, S. Son, Adv. Mater. 32 (2020) 2001945.
[19] L. Li, C.W. Zhang, G.Y. Chen, Nat. Commun. 5 (2014) 3276.
[20] J. Huang, D. Hong, W. Lang, Analyst 144 (2019) 3703–3709.
[21] L. Gao, W. Wang, X. Wang, Chem. Soc. Rev. 50 (2021) 1219–1250.
[22] X. Wu, W. Shi, X. Li, Angew. Chem. Int. Ed. 56 (2017) 15319–15323.
[23] Z. Yang, W. Li, H. Chen, Chem. Comm. 55 (2019) 2477–2480.
[24] H. Fang, H. Zhang, L. Li, Angew. Chem. Int. Ed. 59 (2020) 7536–7541.
[25] W. Shen, J. Yu, J. Ge, ACS Appl. Mater. Interfaces 8 (2016) 927–935.
[26] X. Wu, L. Li, W. Shi, Anal. Chem. 88 (2016) 1440–1446.
[27] Z.M. Yang, Q.Y. Mo, J.M. He, ACS Sens. 5 (2020) 943–951.
[28] J. Shang, W. Shi, X. Li, Anal. Chem. 93 (2021) 4285–4290.
[29] J.R. Zheng, S.M. Feng, S.Y. Gong, Sens. Actuators B: Chem. 309 (2020) 127796.
[30] J.X. Hong, W.Y. Feng, G.Q. Feng, Sens. Actuators B: Chem. 262 (2018) 837–844.
[31] D.L. Murphy, F. Karoum, D. Pickar, J. Neural. Transm. Suppl. 52 (1998) 39–48.
[32] P. Severino, A. D'Amato, M. Pucci, et al., Int. J. Mol. Sci. 21 (2020) 3167.
[33] Y. Liu, X.D. Song, W. Liu, J. Cell. Mol. Med. 7 (2003) 49–56.
[34] M.A. Churchward, D.R. Tchir, K.G. Todd, Mol. Neurobiol. 55 (2018) 1477–1487.
[35] P. Krenek, J. Kmecova, D. Kucerova, Eur. J. Heart Fail. 11 (2009) 140–146.
[36] D. Fitchett, S.E. Inzucchi, C.P. Cannon, Circulation 139 (2019) 1384–1395.